

Chemical and Mutagenic Investigations of Fatty Acid Amide Hydrolase: Evidence for a Family of Serine Hydrolases with Distinct Catalytic Properties[†]

Matthew P. Patricelli, Martha A. Lovato, and Benjamin F. Cravatt*

The Skaggs Institute for Chemical Biology and Department of Cell Biology, The Scripps Research Institute, 10666 North Torrey Pines Road, La Jolla, California 92037

Received March 18, 1999; Revised Manuscript Received June 2, 1999

ABSTRACT: Fatty acid amide hydrolase (FAAH) is a membrane-bound enzyme responsible for the catabolism of neuromodulatory fatty acid amides, including anandamide and oleamide. FAAH's primary structure identifies this enzyme as a member of a diverse group of alkyl amidases, known collectively as the "amidase signature family". At present, this enzyme family's catalytic mechanism remains poorly understood. In this study, we investigated the catalytic features of FAAH through mutagenesis, affinity labeling, and steady-state kinetic methods. In particular, we focused on the respective roles of three serine residues that are conserved in all amidase signature enzymes (S217, S218, and S241 in FAAH). Mutation of each of these serines to alanine resulted in a FAAH enzyme bearing significant catalytic defects, with the S217A and S218A mutants showing 2300- and 95-fold reductions in k_{cat} , respectively, and the S241A mutant exhibiting no detectable catalytic activity. The double S217A:S218A FAAH mutant displayed a 230 000-fold decrease in k_{cat} , supporting independent catalytic functions for these serine residues. Affinity labeling of FAAH with a specific nucleophile reactive inhibitor, ethoxy oleoyl fluorophosphonate, identified S241 as the enzyme's catalytic nucleophile. The pH dependence of FAAH's k_{cat} and k_{cat}/K_m implicated a base involved in catalysis with a pK_a of 7.9. Interestingly, mutation of each of FAAH's conserved histidines (H184, H358, and H449) generated active enzymes, indicating that FAAH does not contain a Ser-His-Asp catalytic triad commonly found in other mammalian serine hydrolytic enzymes. The unusual properties of FAAH identified here suggest that this enzyme, and possibly the amidase signature family as a whole, may hydrolyze amides by a novel catalytic mechanism.

Fatty acid amide hydrolase (FAAH)¹ (1) is the only characterized mammalian member of a large family of amidase enzymes termed the "amidase signature" family. This enzyme family is defined by a highly conserved linear sequence rich in serine and glycine residues which spans nearly 50 amino acids in length (Figure 1) (2, 3). More than 45 proteins containing the amidase signature sequence have been identified to date, including in addition to FAAH, many prokaryotic (3–9) and fungal enzymes (10–12), 1 avian enzyme (13), and 3 putative members from *C. elegans*. Despite the presence of amidase signature enzymes in several kingdoms of life, little is presently known about their tertiary structure and/or catalytic mechanism.

Among the amidase signature enzymes, FAAH is of particular interest due to the intriguing biological activities of its fatty acid amide substrates. Several fatty acid amides, including the neuromodulatory compounds anandamide and oleamide, have recently been identified as important mammalian signaling molecules (14–18). Anandamide (arachidonoyl ethanolamide) was first characterized as an endogenous brain ligand for the CB1 cannabinoid receptor (15) and has since been found to possess cannabinoid-like properties in vivo, including induction of hypothermia, analgesia, and memory defects (19). Oleamide (9-*Z*-octadecenamide) was isolated from the cerebrospinal fluid of sleep-deprived cats (20, 21) and shown to induce physiological sleep when injected into rats (14). More recently, oleamide has been found to modulate both serotonergic (22–24) and GABAergic receptor systems (25–26). Both anandamide and oleamide also block intercellular communication through gap junctions (27–29). Finally, a number of other endogenous fatty acid amides have been characterized (17, 30–32), including palmitoyl ethanolamide, a ligand for CB2-like cannabinoid receptors that may act cooperatively with anandamide in the control of peripheral pain responses (32).

[†] This work was supported by grants from the NIH (MH58542), the Skaggs Institute for Chemical Biology, the Searle Scholars Program (B.F.C.), and the National Science Foundation (M.P.P. and M.A.L.).

* Corresponding author: 10550 N. Torrey Pines Rd, La Jolla, CA 92037. Telephone: (619) 784-8633. Fax: (619) 784-2345. Email: cravatt@scripps.edu.

¹ Abbreviations: FAAH, fatty acid amide hydrolase; EOFP, ethoxy oleoyl fluorophosphonate; MAFP, methyl arachidonoyl fluorophosphonate; CD, circular dichroism; HPLC, high-pressure liquid chromatography; EDTA, ethylenediaminetetraacetic acid; SDS, sodium dodecyl sulfate.

FAAH:	215	GGSSGG EGALIGSGGSPLGL GT DIG SSIR FFSAFCGIC GLKPT	257
VDHAP:	223	GGSSGG EGALIAGGGSLLGIGSDVAG SSIR LFSSFCGL CLKPT	265
IAAH:	144	GGSSGG SAAAVASGIVPLSVGTDTG SSIR IPAAFCGIT GF RPT	186
GluAT:	152	GGSSGG SAAAVAAGEVPFSLGSDTG SSIR QPASFCGVV CLKPT	194
AMD:	202	GGSSGG EGAIVGIRGGVIGVGTDTIG SSIR VPAAFNFLY CL RPS	244
RhoJ1:	169	GGSSGG SGALVASGQVDMAVCGDQ GGSSIR IPAAFCGIV CH KPT	211
NicAm:	147	GGSSGG SGAAVAAGVVHVALGSDTG SSIR IPAAALCGTV CL KPT	189
NylAm:	148	GGSSGG SGAAVAAALSPVAHCND AAGSV RI PAS VCGVV CL KPT	190
Urea:	151	GGSSGG SGSVVARGIACALALTDT AGSTR VPAAALNNLISIK PS	193

FIGURE 1: Amidase signature sequences. Selected examples of the amidase signature regions from several amidase signature enzymes. FAAH: fatty acid amide hydrolase, *Rattus norvegicus* (gi:1680722). VDHAP: vitamin D₃ hydroxylase associated protein, *Gallus domesticus* (gi: 1079452). IAAH: indoleacetamide hydrolase, *Pseudomonas syringae* (gi: 77820). GluAT: Glu-tRNA^{glu} amidotransferase, *Bacillus subtilis* (gi: 2589195). AMD: acetamidase, *Emericella nidulans* (gi: 101782). RhoJ1: J1 amidase, *Rhodococcus rhodochrous* (gi: 563984). NicAm: nicotinamidase, *Mycobacterium smegmatis* (gi: 3869278). NylAm: 6-aminohexanoate cyclic dimer hydrolase, *Flavobacterium* sp. (gi: 148711). Urea: urea amidolyase, *Pichia jadinii* (gi: 742250).

The intriguing effects of fatty acid amides on pain, sleep, and memory systems suggest that FAAH might serve as an attractive target for pharmacological efforts aimed at influencing these physiological processes. Indeed, FAAH is abundantly expressed in several neuronal types throughout the central nervous system (33, 34), indicating that this enzyme is poised to terminate the signaling function of its fatty acid amide substrates at their presumed sites of action in vivo. Further support for the role of FAAH in regulating fatty acid amide activity in vivo has derived from experiments showing that FAAH-resistant analogues of anandamide display enhanced pharmacological activity (32, 35). While several potent FAAH inhibitors have been identified (36–38), these compounds tend to suffer from a lack of target specificity, often displaying significant inhibition of enzymes such as phospholipase A₂ as well (39, 40). The poor selectivity of such inhibitors abrogates their use in vivo as agents to study fatty acid amide-based physiological processes. The elucidation of FAAH's catalytic mechanism would likely provide a foundation for the future design of FAAH-specific inhibitors.

In our continued efforts to understand FAAH's structure and function, we have engineered a truncated form of the enzyme lacking its N-terminal transmembrane domain (41). Characterization of this transmembrane domain-deleted, or Δ TM-, FAAH revealed that the enzyme displayed nearly identical catalytic properties to those of wild-type FAAH, and, surprisingly, still associated with membranes despite lacking FAAH's single predicted membrane spanning domain. Δ TM-FAAH was efficiently expressed in *E. coli* and could be solubilized and purified in the presence of detergents. The ability to obtain large quantities of purified Δ TM-FAAH provided us with the opportunity to investigate in detail the catalytic features of this mammalian enzyme.

To date, the nature of FAAH's catalytic residues has remained unclear, with the enzyme displaying sensitivity to both serine- and cysteine-directed inhibitors (37, 38). A comparative analysis of the primary structures of amidase signature enzymes has revealed three completely conserved serine residues, all residing within the signature sequence itself. Interestingly, two of these serines are part of conserved GX SXG motifs, often a characteristic feature of serine hydrolase nucleophiles (42). Recently, one of these three serine residues was mutagenized to alanine in the *Rhodococcus* J1 amidase, resulting in an inactive enzyme (43). However, this study did not investigate the function that this

serine residue played in catalysis, nor was the catalytic importance of the other two conserved serine residues addressed. We now describe the use of mutagenesis, chemical labeling, and steady-state kinetic methods to investigate FAAH's catalytic mechanism and report for the first time that serine residue 241 acts as the enzyme's catalytic nucleophile.

EXPERIMENTAL PROCEDURES

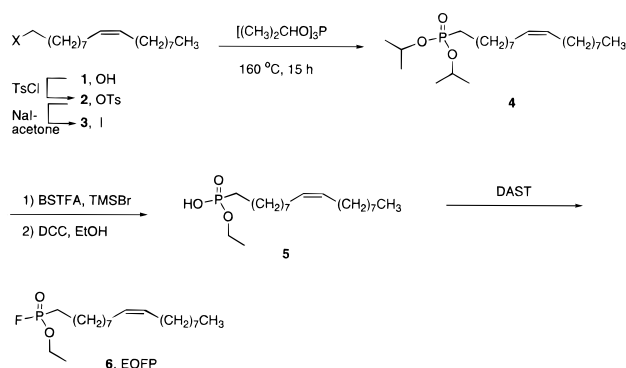
Expression and Purification of FAAH and Mutants. FAAH and other mutant enzymes were expressed in *E. coli* with a His₆ tag and purified by metal affinity, heparin agarose, and gel filtration chromatography as described previously (41). Unless otherwise stated, all expressed proteins could be obtained in purified form at levels approximating 0.5–2.0 mg of protein/L of culture volume. Point mutants were generated using the Quickchange procedure (Stratagene). All mutant cDNAs were sequenced and found to contain only the desired mutation(s).

Affinity Labeling. Routes for the chemical syntheses of ethoxy oleoyl fluorophosphonate (EOFP) and ¹⁴C-EOFP are described below. In typical labeling experiments, 0.1–1.0 mg of FAAH or the indicated mutant was incubated with 5–10 equiv of EOFP at enzyme concentrations of 3–15 μ M in 20 mM Hepes, pH 7.8, 10% glycerol, 1% Triton X-100, 150 mM NaCl, 1 mM EDTA. After 0.5–2.0 h, 1 volume of 2 \times SDS loading buffer (reducing) was added, and the proteins were run on an 8% Tris-Glycine gel (Novex). Labeling experiments with ¹⁴C-EOFP were conducted in a similar manner, except each protein sample (50 μ g) was precipitated with trichloroacetic acid, resuspended in SDS-loading buffer, and run on a 10% Tris-Glycine gel. The gel was then dried and exposed to a phosphorimager screen (Packard) for 2 weeks.

Chemical Synthesis of Ethoxy Oleoyl Fluorophosphonate (EOFP). The synthesis of ethoxy oleoyl fluorophosphonate (EOFP), or 1-(fluoroethoxyphosphinyloxy)-9(Z)-octadecene, was achieved in five steps starting from commercially available oleoyl alcohol. Key intermediates in the synthesis were characterized by nuclear magnetic resonance (NMR) and high-resolution mass spectrometry (FABHRMS). Compound numbers in boldface refer to structures shown in Scheme 1.

1-[(p-Toluenesulfonyl)oxy]-9(Z)-octadecenol (2). A solution of oleoyl alcohol **1** (1.0 g, 3.7 mmol, 1.0 equiv) in pyridine (9.0 mL, 112 mmol, 30 equiv) was cooled to 0 °C

Scheme 1



and treated with *p*TsCl (0.89 g, 4.7 mmol, 1.25 equiv). The reaction mixture was kept at 0°C for 10 h and then partitioned between ethyl acetate (200 mL) and water (200 mL). The organic layer was washed with 10% aqueous HCl (2×200 mL) and saturated aqueous NaCl (200 mL), dried (Na_2SO_4), and concentrated under reduced pressure. Chromatography (SiO_2 , 5×10 cm, 2% ethyl acetate–hexanes) afforded **2** (0.57 g, 1.57 g theoretical, 36.4%) as a colorless oil: ^1H NMR (CDCl_3 , 250 MHz) δ 7.76 (d, $J = 6.5$ Hz, 2H, ArH), 7.32 (d, $J = 7.3$ Hz, 2H, ArH), 5.32 (m, 2H, $\text{CH}=\text{CH}$), 3.98 (t, $J = 6.5$ Hz, 2H, CH_2OTs), 2.42 (s, 3H, ArCH_3), 1.98 (m, 4H, $\text{CH}_2\text{CH}=\text{CHCH}_2$), 1.60 (p, $J = 7.0$ Hz, 2H, $\text{CH}_2\text{CH}_2\text{OTs}$), 1.50–1.20 (m, 22H), 0.85 (t, $J = 6.3$ Hz, 3H, CH_3); FABHRMS (NBA-NaI) m/z 455.2765 ($\text{C}_{25}\text{H}_{42}\text{O}_3\text{S} + \text{Na}^+$ requires 445.2752).

1-Iodo-9(Z)-octadecene (3). A solution of **2** (0.57 g, 1.36 mmol, 1.0 equiv) in acetone (6.8 mL, 0.2 M) was treated with NaI (0.41 g, 2.72 mmol, 2.2 equiv) and the reaction mixture was stirred at reflux for 2 h, producing a yellow–orange solution. The reaction mixture was partitioned between ethyl acetate (200 mL) and water (200 mL). The organic layer was washed sequentially with saturated aqueous $\text{Na}_2\text{S}_2\text{O}_3$ (100 mL) and saturated aqueous NaCl (100 mL), dried (Na_2SO_4), and concentrated under reduced pressure. Chromatography (SiO_2 , 5×10 cm, 2% ethyl acetate–hexanes) afforded **3** (0.46 g, 0.51 g theoretical, 89.9%) as a colorless oil: ^1H NMR (CDCl_3 , 250 MHz) δ 5.33 (m, 2H, $\text{CH}=\text{CH}$), 3.16 (t, $J = 7.0$ Hz, 2H, CH_2I), 1.99 (m, 4H, $\text{CH}_2\text{CH}=\text{CHCH}_2$), 1.80 (p, $J = 6.9$ Hz, 2H, $\text{CH}_2\text{CH}_2\text{I}$), 1.50–1.20 (m, 22H), 0.85 (t, $J = 6.3$ Hz, 3H, CH_3).

1-[Bis(isopropoxy)phosphinyl]-9(Z)-octadecene (4). Triisopropyl phosphite (3.0 mL, 12.2 mmol, 10 equiv) was added to **3** (0.46 g, 1.22 mmol, 1.0 equiv), and the mixture was heated to 160°C for 15 h. Direct chromatography (SiO_2 , 5×10 cm, 10–25% ethyl acetate–hexanes gradient elution) separated the majority of excess triisopropyl phosphite from the reaction product. A second chromatography step (SiO_2 , 5×10 cm, 10–25% ethyl acetate–hexanes gradient elution) afforded **4** (0.36 g, 0.51 g theoretical, 70.8%) as a colorless oil: ^1H NMR (CDCl_3 , 250 MHz) δ 5.31 (m, 2H, $\text{CH}=\text{CH}$), 4.65 (m, 2H, $(\text{CH}_3)_2\text{CHOP}$), 1.96 (m, 4H, $\text{CH}_2\text{CH}=\text{CHCH}_2$), 1.53–1.24 (m, 38H), 0.85 (t, $J = 6.3$ Hz, 3H, CH_3); MALDI–FTMS (DHB) m/z 439.3311 ($\text{C}_{24}\text{H}_{49}\text{O}_3\text{P} + \text{Na}^+$ requires 439.3317).

1-(Hydroxyethoxyphosphinyl)-9(Z)-octadecene (5). A solution of compound **4** (0.36 g, 0.86 mmol, 1.0 equiv) in CH_2Cl_2 (3.5 mL, 0.2 M) was treated dropwise with bis-(trimethylsilyl)trifluoroacetamide (BSTFA, 0.46 mL, 1.72

mmol, 2.0 equiv), followed by dropwise addition of trimethylsilyl bromide (TMSBr, 0.38 mL, 2.90 mmol, 3.3 equiv). The reaction was stirred at room temperature for 20 h, subsequently quenched with 9 mL of 5% (w/v) KHSO_4 , and stirred vigorously for 15 min. The reaction mixture was partitioned between ethyl acetate (100 mL) and water (100 mL). The combined organic layer was washed with saturated aqueous NaCl (200 mL), dried (Na_2SO_4), and concentrated under reduced pressure. The remaining residue was dissolved in pyridine (4.0 mL), and 1.0 mL of this solution was treated with dicyclohexylcarbodiimide (DCC, 0.044 g, 0.21 mmol, 1.0 equiv) followed by ethanol (0.012 mL, 0.21 mmol, 1.0 equiv). The reaction was stirred at room temperature for 6 h after which an additional equivalent of both DCC and ethanol was added. After being stirred an additional 12 h, the reaction mixture was partitioned between ethyl acetate (100 mL) and water (100 mL). The organic layer was washed sequentially with 5% KHSO_4 (2×100 mL) and saturated aqueous NaCl, dried (Na_2SO_4), and concentrated under reduced pressure. Chromatography (SiO_2 , 2×8 cm, 20% CH_3OH – CHCl_3 with 1% aqueous NH_4OH) afforded **5** (0.032 g, 0.103 g theoretical, 30.8%) as a clear oil: ^1H NMR (CDCl_3 , 250 MHz) δ 7.45 (bs, 1H, OH), 5.31 (m, 2H, $\text{CH}=\text{CH}$), 3.91 (m, 2H, $\text{CH}_3\text{CH}_2\text{O}$), 1.97 (m, 4H, $\text{CH}_2\text{CH}=\text{CHCH}_2$), 1.53–1.24 (m, 29H), 0.85 (t, $J = 6.3$ Hz, 3H, CH_3); FABHRMS (NBA-NaI) m/z 383.2681 ($\text{C}_{20}\text{H}_{41}\text{O}_3\text{P} + \text{Na}^+$ requires 383.2691).

EOPF, or 1-(Fluoroethoxyphosphinyl)-9(Z)-octadecene (6). A solution of **5** (0.0147 g, 0.041 mmol, 1.0 equiv) in CH_2Cl_2 (0.4 mL, 0.1 M) at -78°C was treated dropwise with (diethylamino)sulfur trifluoride (DAST, 0.011 mL, 0.082 mmol, 2.0 equiv) and stirred for 10 min. The entire reaction mixture was then chromatographed (SiO_2 , 0.5×5 cm, 20% ethyl acetate–hexanes), affording **6** as a colorless oil (0.011 g, 0.015 g theoretical, 73.3%): ^1H NMR (CDCl_3 , 400 MHz) δ 5.32 (m, 2H, $\text{CH}=\text{CH}$), 4.23 (m, 2H, $\text{CH}_3\text{CH}_2\text{O}$), 2.0 (m, 4H, $\text{CH}_2\text{CH}=\text{CHCH}_2$), 1.85–1.24 (m, 29H), 0.85 (t, $J = 6.3$ Hz, 3H, CH_3); FABHRMS (NBA-NaI) m/z 385.2659 ($\text{C}_{20}\text{FH}_{40}\text{O}_2\text{P} + \text{Na}^+$ requires 385.2648).

For ^{14}C -EOPF, the synthesis was conducted as above, except during the synthesis of compound **5**, where ^{14}C -ethanol (1.0 mCi/mmol, Moravek) was used in place of nonradioactive ethanol. The yield of ^{14}C -EOPF was estimated by liquid scintillation counting relative to known amounts of ^{14}C -ethanol.

Isolation of Labeled Peptides. Protein bands of labeled and unlabeled FAAH samples were excised from SDS–PAGE gels and digested with sequencing grade modified trypsin (Promega), and the resulting peptides were extracted as described by Williams, LoPresti, and Stone (44). Cysteine residues were modified with iodoacetic acid (44). The peptide extracts were evaporated under nitrogen and resuspended in 50% methanol for reverse-phase high-pressure liquid chromatography (HPLC) analysis. The digests were separated using an HP 1100 series HPLC with a Vydac C18 protein and peptide column equilibrated in 98.5% buffer A [H_2O , 0.1% trifluoroacetic acid (TFA)], 1.5% buffer B (CH_3CN , 0.08% TFA). The peptides were eluted with the following gradient: 0–60 min (1.5–30% buffer B), 60–90 min (30–60% buffer B), 90–105 min (60–80% buffer B), 105–110 min (80–100% buffer B). Peaks of interest were collected manually and subjected to mass spectrometric analysis.

Electrospray Mass Spectrometry. Peptide masses were determined using a Sciex API III triple quadrupole mass spectrometer with an ion-spray atmospheric pressure ionization source. Samples were ionized at a positive potential of 4700 V and an orifice potential of 110 V. Spectra were acquired by scanning quadrupole 1 from m/z 500 to 2400 with a scan step of 0.5. The electrospray ionization (ESI) tandem mass spectrometry experiments were performed on a Finnigan LCQ quadrupole ion trap mass spectrometer. The samples were ionized at a positive potential of 4000 V.

Enzyme Assays. Enzyme activity was determined using ^{14}C -oleamide as a substrate as described previously (41). Briefly, the conversion of ^{14}C -oleamide to ^{14}C -oleic acid was quantitated using a phosphorimager (Packard) following the extraction and separation of the radiolabeled compounds by TLC. All reactions were conducted in the presence of 0.04% Triton X-100 as a detergent. We have found the presence of detergent to be necessary for the solubility of FAAH (both wild type and transmembrane domain-deleted). Due to the low activity of the S217A mutant, enzyme concentrations up to 2 μM were required for K_m and k_{cat} determinations. Reactions were monitored for up to 1 h with substrate concentrations ranging from 20 to 100 μM . Reactions with the S217A:S218A mutant were conducted with 10 μM enzyme and 100 μM oleamide. Time courses of up to 8.5 h were monitored, and linear kinetics were obtained in all cases. The error values reported reflect the sample standard deviation of at least four independent trials. For k_{cat} calculations, enzyme concentrations were estimated assuming an absorbance at 280 nm of 0.8 AU for a 1 mg/mL solution of FAAH (41). Errors reported for k_{cat} do not account for possible errors in enzyme concentration or variation between enzyme preparations. In all cases, however, multiple enzyme preparations were tested, and the variation in k_{cat} between independent preparations was less than 20%. Studies of pH-rate dependence were conducted using a reaction buffer of 50 mM Bis-Tris Propane, 50 mM CAPS, 50 mM citrate, 150 mM NaCl. The pH of the buffer was adjusted using NaOH or HCl. The data were fit to the following equation using nonlinear least-squares analysis: $k_{\text{cat}} = (k_{\text{cat}}^1/[\text{H}^+]) / (K_a + [\text{H}^+]) + (k_{\text{cat}}^2/K_a) / (K_a + [\text{H}^+])$ where k_{cat}^1 is the maximal rate of the fully protonated state and k_{cat}^2 is the maximal rate of the deprotonated state (45). The k_{cat} value at pH 10.0 was not used for fitting purposes as FAAH activity began to decrease significantly at this pH.

Circular Dichroism Spectrometry. Protein samples for circular dichroism (CD) measurements were exchanged into a buffer containing 10 mM Tris, pH 8.0, 100 mM NaCl, 0.05% lauryldimethylamine oxide (LDAO) on a Superdex 200 (Amersham/Pharmacia) gel filtration column at a flow rate of 0.5 mL/min. Samples were diluted to an A_{280} of 0.3 (5.75 μM), and CD measurements were recorded at 25 $^\circ\text{C}$ in a 0.1 cm cell on an Aviv stopped-flow CD spectrometer.

RESULTS

In the studies described below, a rat FAAH protein lacking its N-terminal 39 amino acids was used. This modification removed FAAH's predicted N-terminal transmembrane domain, the deletion of which was previously found to leave FAAH's catalytic properties unaltered, while at the same time facilitating the enzyme's purification (41). For the sake of

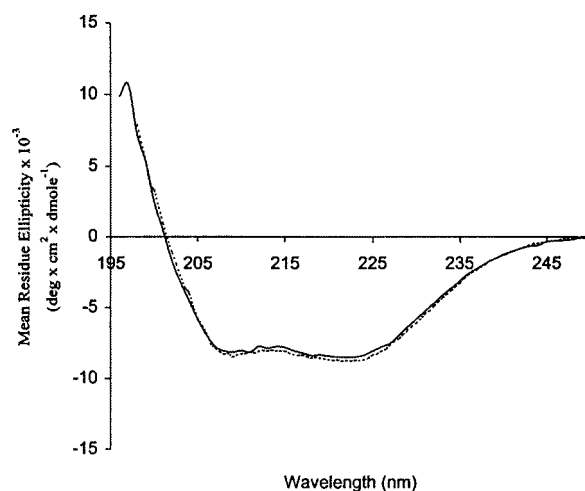


FIGURE 2: Circular dichroism spectra of FAAH and the S241A mutant. The far-UV CD spectra are shown for FAAH (solid line) and the S241A mutant (dashed line). The CD spectra of the S217A, S218A, and S217A:S218A mutants were within error of the spectra shown but were omitted for clarity.

Table 1: Kinetic Properties of FAAH Mutants at pH 9.0

	K_m (μM)	k_{cat} (s^{-1})	k_{cat}/K_m ($\text{M}^{-1} \text{s}^{-1}$)
FAAH	11 ± 3	5.2 ± 0.7	4.7×10^5
S218A	7 ± 1	$(5.5 \pm 0.3) \times 10^{-2}$	7.8×10^3
S217A	15 ± 3	$(2.2 \pm 0.2) \times 10^{-3}$	1.5×10^2
S217A:S218A	ND ^a	$(2.3 \pm 0.1) \times 10^{-5}$ ^b	ND
S241A	ND	$< 5 \times 10^{-6}$	ND
H184Q	30 ± 7	20 ± 2	6.7×10^5
H358A	15 ± 5	4.4 ± 0.5 ^c	2.9×10^5
H449A	29 ± 12	7.7 ± 0.7	2.7×10^5

^a ND, not determined. ^b This k_{cat} value was calculated assuming $V = V_{\text{max}}$ at 100 μM oleamide. ^c This k_{cat} value is based on a concentration of the mutant enzyme estimated from Western blot calibrations with known amounts of FAAH.

clarity, when residue numbers are indicated, they refer to the positions in the full-length FAAH protein.

Kinetic Properties of FAAH Mutants. A comparative analysis of the primary structures of amidase signature enzymes has revealed three completely conserved serine residues (2), all residing within the signature sequence itself. We designed and expressed mutants of FAAH in which each of these serine residues (S217, S218, and S241) was mutated to alanine. The gel filtration elution profiles (data not shown) and circular dichroism spectra of these mutant proteins were not significantly different from those of FAAH (Figure 2), indicating that no major structural changes had occurred as a result of these mutations. Interestingly, kinetic analyses revealed that each serine mutant exhibited a substantial catalytic deficiency relative to FAAH (Table 1). The S217A and S218A mutants possessed k_{cat} values 2300- and 95-fold lower than the k_{cat} of FAAH, respectively, while the S241A mutant showed no detectable catalytic activity. The S217A and S218A mutants displayed no significant changes in their K_m values for oleamide, indicating that these residues are not involved in substrate binding. With respect to the S241A mutant, we estimate conservatively that the lower detection limit for our FAAH activity assay was (1×10^6)-fold below that of wild-type activity, setting a maximal k_{cat} value for this mutant of $5 \times 10^{-6} \text{ s}^{-1}$ (assuming no change in K_m).

Due to the proximity of S217 and S218 in FAAH's primary structure, the possibility was considered that these

residues might function in a coordinated or complementary fashion, perhaps allowing for compensation by one residue in the absence of the other. In this case, the relative importance of these two residues would have been obscured in the above mutagenic analysis. To determine whether S217 and S218 function independently or cooperatively, a mutant enzyme was generated in which both S217 and S218 were replaced with alanine. The enzymatic activity of this double mutant, S217A:S218A, was significantly lower than either S217A or S218A (Table 1). The extremely low activity of this mutant prevented the establishment of a K_m value since the high enzyme concentrations required to detect activity ($10\ \mu\text{M}$) were only 10–15-fold lower than the solubility limit of the substrate, oleamide. Assuming the S217A:S218A mutant did not have a significantly different K_m for oleamide than either single serine mutant, a k_{cat} value of $2.3 \times 10^{-5}\ \text{s}^{-1}$ was obtained. This k_{cat} matches almost exactly the predicted k_{cat} value if S217 and S218 were to function independently: $[5.2\ \text{s}^{-1}/(2300 \times 95)] = 2.4 \times 10^{-5}\ \text{s}^{-1}$. Thus, it is likely that S217 and S218 possess autonomous catalytic functions, with the role of S217 being of greater significance.

Identification of FAAH's Catalytic Nucleophile. While the above mutagenic analysis of FAAH clearly established an order for the relative catalytic importance of the conserved amidase signature family serine residues, the rather severe catalytic defects associated with each mutant enzyme precluded us from determining with confidence which residue represented FAAH's catalytic nucleophile. Additionally, the aforementioned sensitivity of FAAH to both serine- and cysteine-directed agents demanded that a more functional method be developed for defining the enzyme's nucleophile. One powerful approach to identify an amidase's nucleophile is to covalently modify this residue with a specific inhibitor. Previous studies had shown that methyl arachidonoyl fluorophosphonate (MAFP), a commercially available phospholipase A2 inhibitor, was also a potent irreversible inhibitor of FAAH (38). Given that halophosphonate inhibitors have previously been employed as affinity labels to identify active site nucleophiles in serine hydrolases (46, 47), we initially attempted to use MAFP to chemically identify FAAH's nucleophile. Comparing the peptide profiles of tryptic digests of FAAH both prior to and after labeling with MAFP revealed a dramatic reduction in the level of a single FAAH tryptic peptide following MAFP treatment (data not shown). The mass of this depleted peptide identified it as residues 213–243, a region of FAAH that encompasses the majority of the enzyme's amidase signature sequence. However, repeated attempts failed to recover the MAFP-modified form of this peptide, possibly due in part to the potential instability and/or extreme hydrophobicity of the arachidonoyl group of MAFP. Therefore, we chemically synthesized an alternative fluorophosphonate inhibitor, ethoxy oleoyl fluorophosphonate (EOFP, Scheme 1), which we anticipated would react potently with FAAH's active site nucleophile (Figure 3A), while at the same time avoiding the possible stability problems inherent to MAFP's polyene alkyl chain. Importantly, this synthetic strategy also afforded us the ability to incorporate a radiolabel into the EOFP inhibitor.

EOFP was found to behave as an irreversible inhibitor of FAAH (data not shown), displaying properties indistinguishable from those previously described for MAFP (38). FAAH

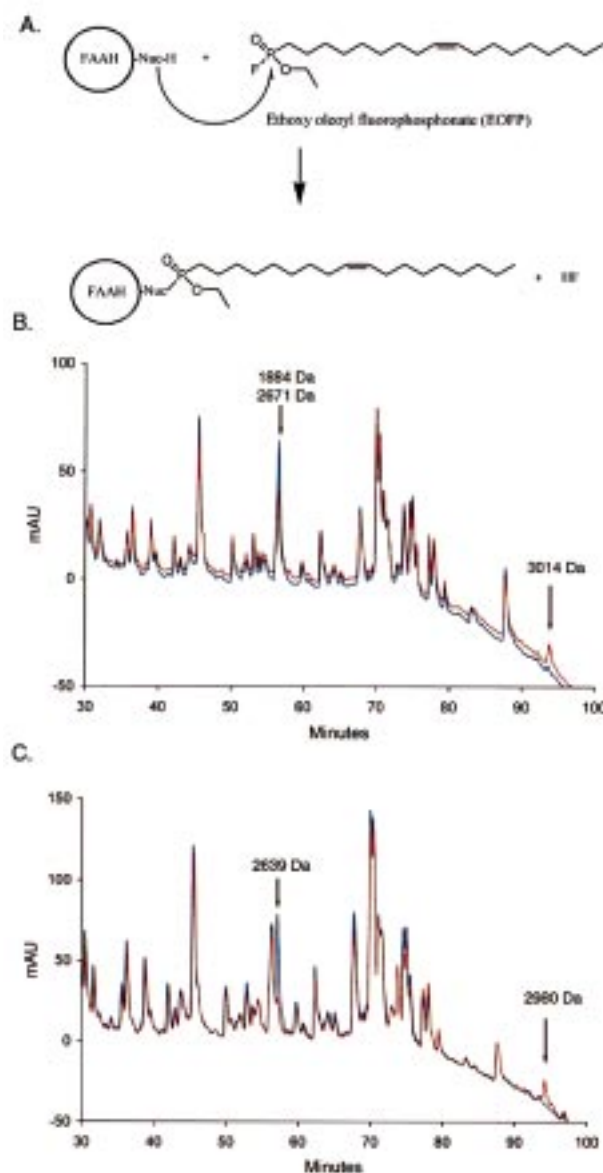


FIGURE 3: Labeling of FAAH with ethoxy oleoyl fluorophosphonate (EOFP). (A) The expected reaction scheme of FAAH with EOFP involves attack by FAAH's nucleophile on the EOFP phosphorus atom, resulting in a covalent enzyme-inhibitor complex. (B) Reverse-phase HPLC of tryptic peptides obtained from FAAH following incubation of the enzyme either in the presence (red trace) or in the absence (blue trace) of EOFP. Electrospray mass spectrometry of the indicated peaks revealed masses corresponding to residues 213–243 (2671 Da) and 244–260 (1885 Da) for the peak at 56.7 min, and residues 213–243 labeled with one molecule of EOFP (3014 Da) for the peak at 94 min. (C) Reverse-phase HPLC of tryptic peptides obtained from the S217A:S218A mutant following incubation of the enzyme either in the presence (red trace) or in the absence (blue trace) of EOFP. Electrospray mass spectrometry of the indicated peaks revealed masses corresponding to residues 213–243 (2639 Da) for the peak at 57.1 min and residues 213–243 labeled with one molecule of EOFP (2980 Da) for the peak at 94 min.

was incubated for 30 min with 0 or 5 equiv of EOFP and then subjected to SDS-PAGE followed by in-gel digestion with trypsin. The resulting tryptic peptides were extracted, concentrated, and separated by reverse-phase HPLC (Figure 3B). Comparison of the HPLC UV absorbance traces for the EOFP-treated and untreated FAAH samples revealed that labeling with EOFP induced (1) a significant decrease in a

peptide peak eluting at 56.7 min, and (2) the appearance of a new peptide peak at 94 min. Electrospray mass spectrometry identified two peptides in the 56.7 min peak with masses of 1884 and 2671 Da, corresponding to amino acids 244–260 and 213–243 of FAAH, respectively. A selective decrease in the mass intensity of the 2671 Da peptide was observed in the EOFP-treated FAAH sample. Mass analysis of the peak eluting at 94 min revealed a single peptide with a mass of 3014 Da, corresponding to the mass of residues 213–243 with an additional 343 Da, the expected additional mass for this peptide modified with one molecule of EOFP.

The EOFP-labeled FAAH peptide contained several highly conserved residues of the amidase signature sequence, including S217, S218, and S241. To identify the exact site of modification, the peptide was first sequenced by Edman degradation. The sequence KSPGGSSGGEGALIGSGGSPLGLGTDIGG was obtained, which corresponds to FAAH residues 213–240 and falls three amino acids short of the expected peptide sequence as predicted by mass analysis. However, only one serine residue, S241, remained in the unsequenced portion of this peptide, suggesting that this residue might be the site of EOFP modification. In support of this notion, Edman degradation has previously been found to stop at phosphorylated serine residues (48, 49). To confirm the position of the modified residue, tandem mass spectrometry was employed on the ethoxy oleoyl phosphonate (EOP)–peptide adduct (Figure 4). Fragmentation of the doubly charged m/z 1507 ion of the labeled peptide yielded several daughter ions which corresponded to the expected peptide fragments for EOFP modification at S241 (Figure 4A). Peaks at m/z 832, 945, 1060, 1218, 1388, 1415, 1598, 1743, 1886, and 1944 all corresponded to fragments 343 mass units larger than predicted for C-terminal fragments of the unmodified FAAH peptide. The smallest of these fragments, m/z 832, corresponded to the sequence IGGSIR with one molecule of inhibitor bound, supporting reaction of EOFP with S241. Peaks at m/z 957, 1070, 1091, 1626, and 1796 corresponded to the predicted masses of unmodified, N-terminal portions of the peptide that lack S241, but collectively contain all of the other serine residues in this peptide.

Several peaks in the daughter ion (MS^2) spectrum did not match the initially predicted fragments of the parent ion. The most prominent daughter ion in this spectrum was a doubly charged ion at m/z 1327. Inspection of other unidentified peaks in the MS^2 spectrum revealed that several peaks, including the m/z 1327 ion, possessed m/z values 17 units below those expected for C-terminal peptide fragments containing an unmodified S241 residue. These fragments likely resulted from cleavage of the modified serine residue at the $C\beta$ – $O\gamma$ bond, releasing the bound inhibitor and leaving a dehydroalanine residue at position 241. Analysis of the daughter ions from the doubly charged m/z 1327 peptide confirmed this possibility (Figure 4B). Daughter ions were generated at m/z 472, 584, 858, 1028, 1235, 1439, 1526, 1584, 1696, 1811, and 1939, all of which matched expected masses for peptides following the loss of the serine hydroxyl at residue 241.

These results clearly demonstrate that S241 of FAAH is labeled by the electrophilic inhibitor EOFP. They do not reveal, however, whether S241 is the only residue in FAAH modified by this agent. To determine whether EOFP modifies

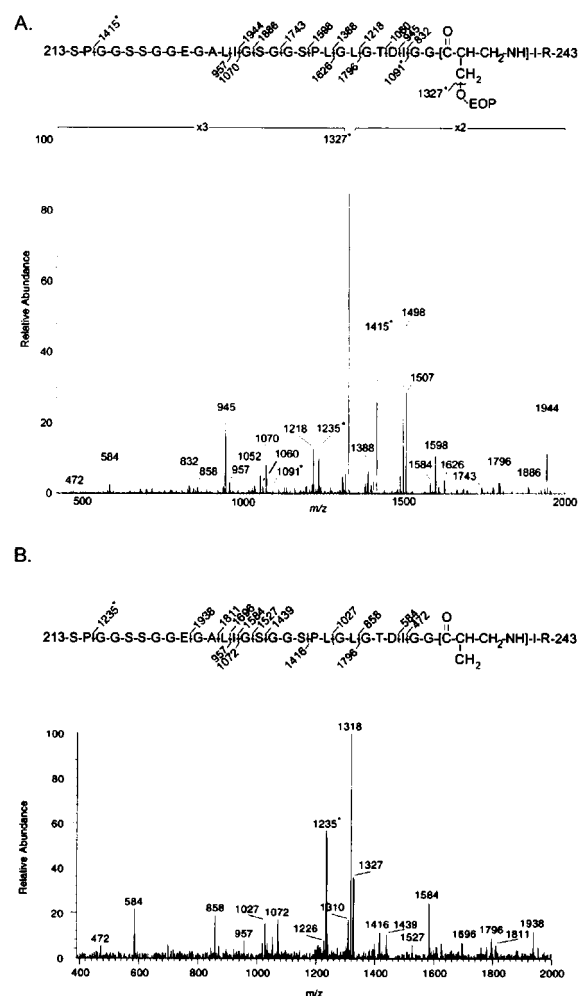


FIGURE 4: Tandem mass spectrometry analysis of the ethoxy oleoyl phosphonate (EOP)–FAAH peptide adduct. (A) MS^2 spectrum of the daughter ions of the doubly charged m/z 1507 EOP–FAAH peptide adduct (corresponding to residues 213–243 of FAAH). The sequence of the peptide and masses of the observed cleavage products are indicated. Numbers above and below the sequence correspond to the m/z values of singly charged C-terminal and N-terminal fragments, respectively. Peaks marked with an asterisk corresponded to doubly charged ions. (B) MS^3 spectrum of the granddaughter ions generated from the doubly charged m/z 1327 daughter ion. The m/z 1327 daughter ion is generated from fragmentation between S241's $C\beta$ and $O\gamma$ atoms, resulting in the release of the bound inhibitor and the generation of a dehydroalanine residue at position 241.

any other residues in FAAH, a ^{14}C -labeled version of EOFP was synthesized. This radioactive inhibitor was incubated with both FAAH and the S241A FAAH mutant for 30 min, after which the protein samples were separated from unbound inhibitor by SDS–PAGE and visualized using a phosphor-imager (Figure 5). While FAAH was clearly labeled with ^{14}C -EOFP and showed no change in labeling intensity with increasing concentrations of inhibitor, no detectable radioactivity was associated with the S241A mutant, even upon incubation with 50 molar equiv of ^{14}C -EOFP. These results indicate that EOFP exclusively modifies FAAH at S241, providing compelling evidence that this residue is FAAH's catalytic nucleophile.

To test whether S217 and/or S218 were necessary for the activation of FAAH's S241 nucleophile, the ability of the S217A:S218A mutant to react with EOFP was assessed. HPLC analyses of tryptic digests of the double mutant

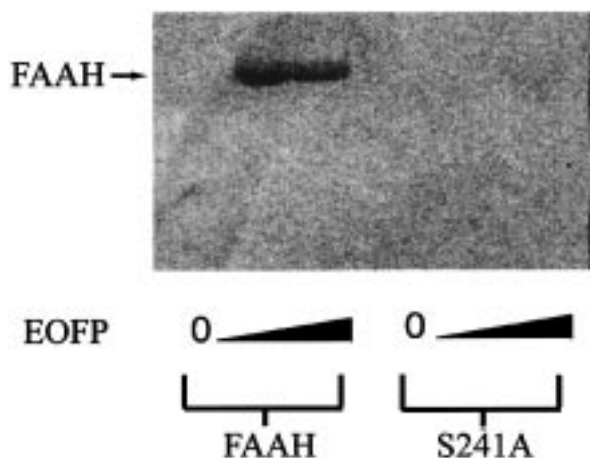


FIGURE 5: Labeling of FAAH with ^{14}C -EOFP. FAAH (left lanes) and the S241A mutant (right lanes) were incubated with increasing concentrations (0, ~ 5 , and ~ 50 equiv) of ^{14}C -EOFP, prior to SDS-PAGE analysis and visualization by phosphorimaging. Radioactive bands corresponding to EOFP-labeled proteins were observed for FAAH, but not for the S241A mutant.

revealed a single UV absorbance peak at 57.1 min that was significantly depleted upon treatment of this enzyme with EOFP (Figure 3C). In the EOFP-treated sample, the appearance of a new UV absorbance peak at 94 min was also observed (Figure 3C). Mass spectrometry analysis of the peak at 57.1 min identified a single peptide with a mass of 2639 Da, matching the expected molecular mass of residues 213–243 of the S217A:S218A mutant. The peak at 94 min contained a peptide with a mass of 2980 Da, corresponding to these same residues modified with one molecule of EOFP. These results show that the S217A:S218A mutant FAAH, despite being catalytically compromised by a factor greater than 10^5 , still reacts with EOFP, indicating that these residues are not required for the activation of FAAH's catalytic nucleophile.

Investigations of FAAH's Catalytic Base. A pH–rate profile of FAAH revealed that the enzyme's k_{cat} increased from pH 5.35 to 9.5 with a sharp drop above pH 10.0 (Figure 6). The enzyme was notably unstable at pH 5.0 and 10.5, and no activity could be detected below pH 4.5 or above pH 11.0. No significant changes were observed in K_m over the measured pH range, meaning that the k_{cat}/K_m profile was essentially identical to the k_{cat} profile. Assuming simple Michaelis-Menten kinetics in the pH range of 5.35–9.5, a basic residue involved in catalysis was observed with a pK_a of 7.9 ± 0.1 . Interestingly, FAAH's pH–rate profile differed significantly from those of most serine proteases, whose histidine bases tend to display pK_a values closer to 7.0 (50).

To test the possibility that a catalytically essential histidine served as FAAH's general base, the three histidine residues which are conserved in rat, mouse, and human FAAHs were independently mutated (H184, H358, and H449; see ref 51). Mutation of H449 to alanine or H184 to glutamine generated enzymes that exhibited similar catalytic properties to those of FAAH (Table 1). Mutation of H184 to alanine resulted in a poorly expressed, but active enzyme which proved unstable to purification (data not shown). Histidine 358, which is conserved in several but not all amidase signature enzymes, appeared to serve a possible structural role as only low quantities (25–50 $\mu\text{g/L}$ culture) of an H358A mutant enzyme could be recovered in soluble form. Still, significant

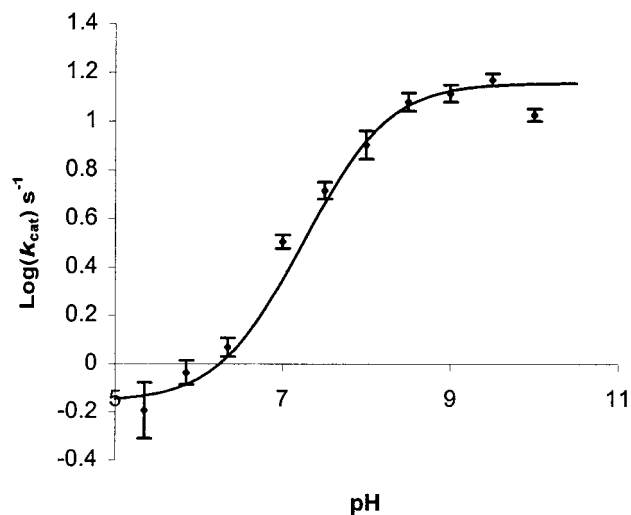


FIGURE 6: pH vs $\log k_{\text{cat}}$ profile of FAAH. The pH dependence of FAAH's k_{cat} is shown with a fit obtained from nonlinear least-squares analysis according to a single residue ionization model. This profile indicates a catalytically important basic residue in FAAH with a pK_a of 7.9 ± 0.1 .

FAAH activity could be detected in lysates from *E. coli* expressing the H358A enzyme, and following partial purification by metal affinity and heparin agarose chromatography steps, this mutant was kinetically characterized. The concentration of the H358A mutant was estimated by comparing samples of this protein to known quantities of FAAH in a Western blot analysis. The H358A mutant's k_{cat} and K_m values were found to be nearly identical to those of FAAH (Table 1). Collectively, the catalytic properties of these histidine mutants indicate that FAAH does not utilize a histidine base for the activation of its serine nucleophile.

DISCUSSION

The mutagenesis and affinity labeling studies presented here clearly demonstrate that S241 serves as FAAH's catalytic nucleophile. When coupled with the observation that this serine residue is conserved in all amidase signature enzymes characterized to date, these data also suggest that this residue may function as the nucleophile for the entire amidase signature family. In support of this notion, the corresponding serine residue in the *Rhodococcus* J1 amidase was recently mutagenized to alanine and shown to result in an inactive enzyme (43). However, unlike FAAH, the J1 amidase is curiously insensitive to serine-directed agents such as DIFP and PMSF (43), possibly indicating that non-serine-based nucleophilic mechanisms might operate in other amidase signature enzymes. Additionally, the J1 amidase exhibits a strong pH dependence of activity from pH 5 to 7 with relatively pH-independent activity from pH 7 to 9 (4), properties that sharply contrast with FAAH's pH–rate profile. Still, such distinguishing features between members of the amidase signature family do not necessarily preclude a shared catalytic mechanism for these enzymes. Indeed, other hydrolytic enzymes such as signal peptidase (52) and pancreatic lipase (53) are not affected by fluorophosphate and sulfonyl fluoride inhibitors despite possessing serine nucleophiles, and it is conceivable that particular members of the amidase signature family might also display such a phenotype. Regarding FAAH's sensitivity to the sulfhydryl-directed agent HgCl_2 (37), we suspect that this compound

may exert its effect on FAAH by inducing gross structural changes in the enzyme. In support of this notion, we have found that incubation of FAAH with HgCl_2 greatly perturbed the quaternary structure of the enzyme as judged by gel filtration (data not shown).

Mutagenesis of S217 and S218 of FAAH, two serine residues that like S241 are conserved in all amidase signature enzymes, revealed that these residues also play significant roles in catalysis. The presence of three serine residues involved in catalysis is highly unusual for an amidase. Among Ser-His-Asp catalytic triad containing serine hydrolases, we identified only the fungal cutinase family of lipase enzymes as having been found to utilize a conserved serine or threonine hydroxyl other than the nucleophilic serine (54). In these enzymes, the nonnucleophilic serine residue's hydroxyl donates a hydrogen bond to the oxyanion of the tetrahedral intermediate (54). The more recently characterized Ser-Lys dyad enzymes such as the class A β -lactamases and *E. coli* signal peptidase have also been found to contain a nonnucleophilic serine residue in their active sites (52, 55). In the class A β -lactamases, this serine is thought to assist in proton transfer to the leaving amide nitrogen of the substrate (55, 56). Finally, the *E. coli* type II asparaginase contains two conserved threonine residues involved in catalysis, with one threonine proposed to serve the role of the nucleophile and the other the role of a base to activate the deacylating water molecule (57). The catalytic defects observed here for the S217A and S218A FAAH mutants are consistent with accessory roles in catalysis such as those discussed above (58, 59) rather than direct catalytic roles such as nucleophile activation (60).

Having determined that FAAH possesses a serine nucleophile, we considered the possibility that this enzyme might contain a Ser-His-Asp catalytic triad analogous to those commonly found in protease active sites (61). Indeed, the identification of a catalytically important basic residue in FAAH with a pK_a of 7.9 was perhaps consistent with this idea. However, the near-wild-type levels of catalytic activity observed for the FAAH mutants H184Q, H358A, and H449A, which constitute the only three conserved histidine residues among rat, mouse, and human FAAHs (51), strongly suggest that a histidine base does not participate in FAAH's catalytic mechanism. Among serine hydrolases, class A β -lactamases (55), the type I signal peptidases (52), and the LexA repressor (62) have been found to utilize a non-histidine base in catalysis. In these unusual cases, a lysine residue is thought to function as the general base to assist in nucleophilic attack by the serine hydroxyl. FAAH possesses three potentially basic residues that are conserved in all amidase signature enzymes characterized to date: K142, D237, and R243. If any one of these residues was to function as FAAH's catalytic base, its pK_a value would have to be shifted 3–5 units. Such large changes in side chain pK_a s are not without precedent, especially within hydrophobic enzyme active sites or when ion pair dipole interactions are present. Further characterization of FAAH's chemical and kinetic mechanism, as well as high-resolution structural studies, will likely be required to determine the potential roles of these residues in FAAH's catalytic mechanism.

Collectively, these studies suggest that the amidase signature family constitutes a unique class of serine hydrolytic enzymes. Members of this enzyme family are present

in several kingdoms of life, where they perform a number of important biological functions (1, 7–9, 10). Amidase signature enzymes display a remarkable variance in their individual substrate selectivities, ranging from glutamine (8) to indoleacetamide (7) to fatty acid amides (1), raising provocative mechanistic and structural questions pertaining to the impressive evolutionary flexibility of this enzyme family. Indeed, strains of *Flavobacterium* and *Pseudomonas* that have adapted to grow on chemicals produced by nylon factories have been found to possess novel amidase signature enzymes capable of selectively hydrolyzing the nylon byproduct, 6-aminohexanoate-cyclic dimer (63). To better appreciate how the amidase signature family has evolved to contain members with such distinct substrate selectivities, more biochemical and structural studies building on the work presented here will be required. Finally, the special catalytic properties exhibited by amidase signature enzymes should also aid in the design of specific inhibitors targeting individual members of this family. Such inhibitors for FAAH would serve not only as valuable research tools, but also as potential therapeutic agents.

ACKNOWLEDGMENT

We thank Phil Dawson and Ashraf Brik for use of and assistance with the Sciex API III mass spectrometer, Gary Siuzdak and Jiang Wu for performing tandem mass spectrometry experiments, Mike Petrassi for assistance with CD measurements, and Jeffery Kelly, Paul Schimmel, Norton Gilula, and Michael Bracey for helpful suggestions with the manuscript.

REFERENCES

- Cravatt, B. F., Giang, D. K., Mayfield, S. P., Boger, D. L., Lerner, R. A., and Gilula, N. B. (1996) *Nature* 384, 83–87.
- Chebrou, H., Bigey, F., Arnaud, A., and Galzy, P. (1996) *Biochim. Biophys. Acta* 1298, 285–293.
- Mayaux, J.-F., Cerbelaud, E., Soubrier, F., Faucher, D., and Petre, D. (1990) *J. Bacteriol.* 172, 6764–6773.
- Kobayashi, M., Komeda, H., Nagasawa, T., Nishiyama, M., Horinouchi, S., Beppu, T., Yamada, H., and Shimizu, S. (1993) *Eur. J. Biochem.* 217, 327–36.
- Hashimoto, Y., Nishiyama, M., Ikehata, O., Horinouchi, S., and Beppu, T. (1991) *Biochim. Biophys. Acta* 1088, 225–233.
- Tsuchiya, K., Fukuyama, S., Kanzaki, N., Kanagawa, K., Negoro, S., and Okada, H. (1989) *J. Bacteriol.* 171, 3187–3191.
- Klee, H., Montoya, A., Horodyski, F., Lichtenstein, C., Garfinkel, D., Fuller, S., Flores, C., Peschon, J., Nester, E., and Gordon, M. (1984) *Proc. Natl. Acad. Sci. U.S.A.* 81, 1728–1732.
- Curnow, A. W., Hong, W., Yuan, R., Kim, S.-I., Martins, O., Winkler, W., Henkin, T. M., and Söll, D. (1997) *Proc. Natl. Acad. Sci. U.S.A.* 94, 11819–11826.
- Boshoff, H. I. M., and Mizrahi, V. (1998) *J. Bacteriol.* 180, 5809–5814.
- Corrick, C. M., Twomey, A. P., and Hynes, M. J. (1987) *Gene* 53, 63.
- Gomi, K., Kitamoto, K., and Kumagai, C. (1991) *Gene* 108, 91–98.
- Genbauffe, F. S., and Cooper, T. G. (1991) *DNA Sequence* 2, 19–32.
- Ettinger, R. A., and DeLuca, H. F. (1995) *Arch. Biochem. Biophys.* 316, 14–19.
- Cravatt, B. F., Prospero-Garcia, O., Siuzdak, G., Gilula, N. B., Henriksen, S. J., Boger, D. L., and Lerner, R. A. (1995) *Science* 268, 1506–1509.

15. Devane, W. A., Hanus, L., Breuer, A., Pertwee, R. G., Stevenson, L. A., Griffin, G., Gibson, D., Mandelbaum, A., Etinger, A., and Mechoulam, R. (1992) *Science* 258, 1946–1949.
16. Facci, L., Dal Toso, R., Romanello, S., Buriani, A., Skaper, S. D., and Leon, A. (1995) *Proc. Natl. Acad. Sci. U.S.A.* 92, 3376–3380.
17. Wakamatsu, K., Masaki, T., Itoh, F., Koichi, K., and Sudo, K. (1990) *Biochem. Biophys. Res. Commun.* 168, 423–429.
18. Barg, J., Frider, E., Hanus, L., Levy, R., Matus-Leibovitch, N., Heldman, E., Bayewitch, M., Mechoulam, R., and Vogel, Z. (1995) *Eur. J. Pharmacol.* 287, 145–152.
19. Smith, P. B., Compton, D. R., Welch, S. P., Razdan, R. K., Mechoulam, R., and Martin, B. R. (1994) *J. Pharmacol. Exp. Ther.* 270, 219–227.
20. Lerner, R. A., Siuzdak, G., Prospero-Garcia, O., Henriksen, S. J., Boger, D. L., and Cravatt, B. F. (1994) *Proc. Natl. Acad. Sci. U.S.A.* 91, 9505–9508.
21. Cravatt, B. F., Lerner, R. A., and Boger, D. L. (1996) *J. Am. Chem. Soc.* 118, 580–590.
22. Hiudobro-Toro, J., and Harris, R. A. (1996) *Proc. Natl. Acad. Sci. U.S.A.* 93, 8078–8082.
23. Thomas, E. A., Carson, M. J., Neal, M. J., and Sutcliffe, J. G. (1997) *Proc. Natl. Acad. Sci. USA* 94, 14115–14119.
24. Boger, D. L., Patterson, J. E., and Jin, Q. (1998) *Proc. Natl. Acad. Sci. U.S.A.* 95, 4102–4107.
25. Yost, C. S., Hampson, A. J., Leonoudakis, D., Koblin, D. D., Bornheim, L. M., and Gray, A. T. (1998) *Anesth. Analg.* 86, 1294–1300.
26. Lees, G., Edwards, M. D., Hassoni, A. A., Ganellin, C. R., and Galanakis, D. (1998) *Br. J. Pharmacol.* 124, 873–882.
27. Venance, L., Piomelli, D., Glowinski, J., and Giaume, C. (1995) *Nature* 376, 590–594.
28. Guan, X., Cravatt, B. F., Ehring, G. R., Hall, J. E., Boger, D. L., Lerner, R. A., and Gilula, N. B. (1997) *J. Cell Biol.* 139, 1785–1792.
29. Boger, D. L., Patterson, J. E., Guan, X., Cravatt, B. F., Lerner, R. A., and Gilula, N. B. (1998) *Proc. Natl. Acad. Sci. U.S.A.* 95, 4810–4815.
30. Di Marzo, V., Fontana, A., Cadas, H., Schinelli, S., Cimino, G., Schwartz, J.-C., and Piomelli, D. (1994) *Nature* 372, 686–691.
31. Arafat, E. S., Trimble, J. W., Andersen, R. A., Dass, C., and Desiderio, D. M. (1989) *Life Sci.* 45, 1679–1687.
32. Calignano, A., La Rana, G., Giuffrida, A., and Piomelli, D. (1998) *Nature* 394, 277–281.
33. Thomas, E. A., Cravatt, B. F., Danielson, P. E., Gilula, N. B., and Sutcliffe, J. G. (1997) *J. Neurosci. Res.* 50, 1047–1052.
34. Egertova, M., Giang, D. K., Cravatt, B. F., and Elphick, M. R. (1998) *Proc. R. Soc. London, Ser. B: Biol. Sci.* 265, 2081–2085.
35. Romero, J., Garcia-Palomero, E., Lin, S. Y., Ramos, J. A., Makriyannis, A., and Fernandez-Ruiz, J. J. (1996) *Life Sci.* 58, 1249–1257.
36. Koutek, B., Prestwich, G. D., Howlett, A. C., Chin, S. A., Salehani, D., Akhavan, N., and Deutsch, D. J. (1994) *J. Biol. Chem.* 269, 22937–22940.
37. Patterson, J. E., Ollman, I. R., Cravatt, B. F., Boger, D. L., Wong, C. H., and Lerner, R. A. (1996) *J. Am. Chem. Soc.* 118, 5938–5945.
38. Deutsch, D. G., Omeir, R., Arreaza, G., Salehani, D., Prestwich, G. D., Huang, Z., and Howlett, A. (1997) *Biochem. Pharmacol.* 53, 255–260.
39. Ackerman, E. J., Conde-Frieboes, K., and Dennis, E. A. (1995) *J. Biol. Chem.* 270, 445–450.
40. Huang, Z., Payette, P., Abdullah, K., Cromlish, W. A., and Kennedy, B. P. (1996) *Biochemistry* 35, 3712–3721.
41. Patricelli, M. P., Lashuel, H. A., Giang, D. K., Kelly, J. W., and Cravatt, B. F. (1998) *Biochemistry* 37, 15177–15187.
42. Brenner, S. (1988) *Nature* 334, 528.
43. Kobayashi, M., Fujiwara, Y., Goda, M., Komeda, H., and Shimizu, S. (1997) *Proc. Natl. Acad. Sci. U.S.A.* 94, 11986–11991.
44. Williams, K., LoPresti, M., and Stone, K. (1997) in *Techniques in Protein Chemistry VIII* (Marshak, D. R., Ed.) pp 79–90, Academic Press, New York.
45. Fersht, A. R. (1985) in *Enzyme Structure and Mechanism*, p 156, W. H. Freeman, New York.
46. Dixon, G., Go, S., and Neurath, H. (1956) *Biochim. Biophys. Acta* 19, 193.
47. Brzozowski, A. M., Derewenda, U., Derewenda, Z. S., Dodson, G. G., Lawson, D. M., Turkenburg, J. P., Bjorkling, F., Hugen-Jensen, B., Patkar, S. A., and Thim, L. (1991) *Nature* 351, 491–494.
48. Jansz, H. S., Posthumus, C. H., and Cohen, J. A. (1959) *Biochim. Biophys. Acta* 33, 396–403.
49. Augusteyn, R. C., de Jersey, J., Webb, E. C., and Zerner, B. (1969) *Biochim. Biophys. Acta* 171, 128–137.
50. Bachovchin, W. W., Kaiser, R., Richards, J. H., and Roberts, J. D. (1981) *Proc. Natl. Acad. Sci. U.S.A.* 78, 7323–7326.
51. Giang, D. K., and Cravatt, B. F. (1997) *Proc. Natl. Acad. Sci. U.S.A.* 94, 2238–2242.
52. Paetzel, M., Dalbey, R. E., and Strynadka, N. C. J. (1998) *Nature* 396, 186–190.
53. Maylie, M. F., Charles, M., and Desnuelle, P. (1972) *Biochim. Biophys. Acta* 276, 162–175.
54. Nicolas, A., Egmond, M., Verrips, C. T., Vlieg, J., Longhi, S., Cambillau, C., and Martinez, C. (1996) *Biochemistry* 35, 398–410.
55. Strynadka, N. C. J., Adachi, H., Jensen, S. E., Johns, K., Sielecki, A., Betzel, C., Sutoh, K., and James, M. N. G. (1992) *Nature* 359, 700–705.
56. Maveyraud, L., Pratt, R. F., and Samama, J.-P. (1998) *Biochemistry* 37, 2622–2628.
57. Palm, G. J., Lubkowski, J., Derst, C., Schleper, S., Rohm, K.-H., and Wlodawer, A. (1996) *FEBS Lett.* 390, 211–216.
58. Bryan, P., Pantoliano, M. W., Quill, S. G., Hsiao, H.-Y., and Poulos, T. (1986) *Proc. Natl. Acad. Sci. U.S.A.* 83, 3743–3745.
59. Jacob, F., Joris, B., Lepage, S., Dusart, J., and Frere, J. M. (1990) *Biochem. J.* 271, 399–406.
60. Carter, P., and Wells, J. A. (1988) *Nature* 332, 564–568.
61. Dodson, G., and Wlodawer, A. (1998) *Trends Biochem. Sci.* 23, 347–352.
62. Lin, L. L., and Little, J. W. (1989) *J. Mol. Biol.* 210, 439–452.
63. Okada, H., Negoro, S., Kimura, H., and Nakamura, S. (1983) *Nature* 306, 203–206.

BI990637Z